LAWRENCE
LIVERMORE
NATIONAL
LABORATORY

LLNL-JRNL-456334

Spin crossover in ferropericlase at high pressure: a seismically silent/transparent transition?

D. Antonangeli, J. Siebert, C. Aracne, D. Farber, A. Bosak, M. Hoesch, M. Krisch, F. Ryerson, G. Fiquet, J. Badro

September 21, 2010

Science

Disclaimer

Spin crossover in ferropericlase at high pressure: a seismically silent/transparent transition?

Daniele Antonangeli[1,2,*], Julien Siebert[1,2], Chantel M. Aracne[2], Daniel L. Farber[2,3], A. Bosak[4], M. Hoesch[4], M. Krisch[4], Frederick J. Ryerson[2], Guillaume Fiquet[1], James Badro[1,2]

[1] *Institut de Minéralogie et de Physique des Milieux Condensés, UMR CNRS 7590, Institut de Physique du Globe de Paris, Université Pierre et Marie Curie, Université Paris Diderot, 75005 Paris, France.*

[2] *Lawrence Livermore National Laboratory, Livermore, California 94550, USA*

[3] *Department of Earth and Planetary Sciences, University of California, Santa Cruz, Santa Cruz, CA, 95064*

[4] *European Synchrotron Radiation Facility, BP 220, 38043 Grenoble Cedex, France*

** To whom correspondence should be addressed. E-mail: daniele.antonangeli@impmc.upmc.fr*

Abstract

Although existing studies indicate a strong influence of the iron spin state transition on the elasticity of ferropericlase, to date, no seismological investigation has reported evidence of an elastic anomaly directly caused by this transition in the lower mantle. Our inelastic x-ray scattering measurements on $(Mg_{0.83}Fe_{0.17})O$ ferropericlase up to 70 GPa show no effect for the longitudinal modulus, C_{11}, only a softening of the shear modulus, C_{44}, along with a small anomaly for C_{12}. This explains the absence of a significant deviation in the aggregate velocities, and thus the lack of a one-dimensional seismic signature due to the spin crossover. However, the elastic shear anisotropies of high-spin and low-spin ferropericlase are profoundly different, and may account for the seismic shear wave anisotropy of the lower mantle.

The characterization of pressure- and temperature-induced transitions of mantle minerals, and their link with seismic discontinuities, is one of the most striking contributions provided by mineral physics for the understanding of Earth's interior. Emblematic in this sense is the series of phase transformations that occurs in olivine, which, with increasing pressure, first transforms to wadsleyite, then to ringwoodite, and then breaks down into ferropericlase and perovskite. These phase changes are accompanied by density and sound velocity variations that ultimately define the main seismic discontinuities of the upper mantle (1).

On the contrary, the recently discovered spin transition in ferropericlase (2) and perovskite (3), the two main phases of the lower mantle, has not yet been clearly related to any seismic signature, even though effects on mantle's density and seismic wave velocity have been anticipated (4-7). With specific regard to ferropericlase, the spin transition occurs without change in the structure (4,8), but experimental (9,10) and theoretical (11) studies indicate large softening of all the elastic moduli and consequently a significant decrease in the aggregate sound velocities. Such an effect should result in a seismic discontinuity or anomaly, albeit broad, depending upon the range of the pressure and temperature over which the spin crossover occurs (12). However, no seismic anomalies are observed at relevant depths (13).

Here we present measurements of the complete elastic tensor of $(Mg_{0.83}Fe_{0.17})O$-ferropericlase up to 70 GPa. These data are then used to estimate the relevant seismic parameters for a ferropericlase-bearing low mantle phase assemblage, and to suggest the type of seismic observations that may be most sensitive to the pressure-induced spin transition.

Inelastic x-ray scattering (IXS) has proven to be an extremely useful technique for the high-pressure study of elasticity and sound velocities of both powders (14-18), and single crystals (19-21). Furthermore, all the independent elements of the elastic tensor can be directly determined from the initial slope of the phonon dispersion of selected longitudinal acoustic and transverse acoustic modes, without any external input or *a priori* model (22),

thus overcoming possible limitations associated with the complex data treatment of impulsive stimulated light scattering (ISLS) measurements (9,23) and the need to use an independently determined bulk modulus to solve for all the elastic moduli having measured only shear velocities (10). This last point is critically important in the mixed spin region.

Oriented single crystals of $(Mg_{1-x}Fe_x)O$ were synthesized by high-temperature Fe-Mg interdiffusion in a pre-aligned crystal of MgO (normal parallel to [110] direction) in a piston-cylinder press. Sample disks with dimensions suited for diamond anvil cell (DAC) experiments (~40 μm diameter, 15-20 μm thick) were prepared using femtosecond laser cutting and mechanical polishing (24). The exact composition was determined individually for each disk by electron microprobe analysis and the ferric/ferrous ratio by electron energy loss spectroscopy (22).

Samples with x=0.17 ($Fe^{3+}/\Sigma Fe$ <2%) were loaded in membrane driven DAC, equipped with rhenium gaskets and either 300 or 250 μm culet diamonds, using neon as pressure transmitting medium to ensure quasi-hydrostatic compression. Three runs were performed to collect data at 1.8, 9, 26, 34, 47, 54, 62 and 70 GPa, as determined by ruby fluorescence. The IXS measurements were performed at the ID28 beamline of the European Synchrotron Radiation Facility. As opposed to Brillouin scattering that is restricted to transparent samples (10, 25, 26), opaque specimens can be investigated by IXS, thus allowing us to look at ferropericlase with 17 at.% Fe, a concentration more relevant to the lower mantle than that used in recent work (6 at.% (9,25) and 10 at.% (10,26)).

The elastic moduli are reported as a function of pressure in Figure 1. Up to ~ 40 GPa, all the moduli exhibit a monotonic increase with pressure, as commonly expected with compression. In the 40 to 60 GPa pressure range, where the spin transition occurs (2,4,28), we observe a distinct softening of C_{44}, and a small anomaly in C_{12}, while C_{11} retains a normal evolution. Above 60 GPa, the usual monotonic increase with pressure is observed by all the

moduli. The back extrapolations of our results to ambient pressure are in good agreement with ultrasonic determinations for the same composition. However, if we compare our high-pressure measurements with ISLS (9) and Brillouin (10, 26) data obtained on samples with lower iron content, we observe a qualitative agreement for C_{44} and $C'=1/2(C_{11}-C_{12})$, which display softening in the pressure range of the spin transition for all methods (quantitative differences are likely due to differences in iron concentration), but disagreement for C_{12} and, most importantly, for C_{11}. Indeed, while both optical studies (9,26) report a large softening of C_{11} in the 40-60 GPa range, the direct determination of C_{11} by IXS (via sound velocity measurements of the LA[100] mode, see 22) does not show any anomaly (Figure 1). To support our findings, we stress that spin-pairing transitions in iron-Invar alloys (as well as in Co- and Mn-Invar alloys) are commonly accompanied by much larger effects on the shear elastic moduli than on the longitudinal moduli (29,30).

From the measured single-crystalline C_{ij} we can compute the aggregate elastic properties (bulk and shear moduli, compressional and shear sound velocities) by simple averaging (22). The values we obtain for the bulk and shear modulus compare favorably with the ambient pressure ultrasonic determination (27) and with the values obtained by x-ray diffraction (4) both for the low spin and the high spin state (Figures S3 and S4).

A direct and very important consequence of the lack of softening of C_{11} and of the quite moderate effect on C_{12}, is the absence of any significant deviation from a linear density evolution of the aggregate compressional (V_P) and shear (V_S) sound velocities (Figure 2). Specifically, neither V_P nor V_S show an anomaly due to the spin-pairing transition, in striking contrast with recent claims (9-11).

With respect to the Earth's lower mantle, recent optical and theoretical studies (9-11) proposed that an anomalous (albeit smooth) softening of the aggregate elastic properties (especially the bulk modulus K and the bulk velocity $V_\Phi=\sqrt{K/\rho}$) should occur at depth. The

range over which this takes place has been suggested to extend from 1000 to 1500 km, based on room-temperature results (9), and from 1300 to 1800 km, when modeling high-temperature effects (10), including those along a mantle geotherm and for a uniform aggregate with pyrolite composition (11). In contrast, there is currently no seismological evidence of such elastic anomalies in this range of depths. Our study provides a clear explanation for this lack of one-dimensional seismic signature associated with the spin crossover in the lower mantle.

The high-spin to low-spin transition does however have an effect on the single-crystal elasticity of ferropericlase. In Figure 3 we illustrate the pressure evolution of the shear elastic moduli C_{44} and C', corresponding to the sound velocity of the $TA[110]_{<001>}$ and $TA[110]_{<-110>}$ modes respectively. In agreement with Brillouin determination on samples with 10 at.% Fe content (10, 26), we observe $C_{44} > C'$ at ambient and low pressures, but the pressure derivative of C' is larger than that of C_{44}, so that the two cross around 16-17 GPa, and at higher pressures the sign of shear anisotropy is reversed. Above 60 GPa, in the low spin phase, the pressure derivative of the two shear moduli is almost the same. Accordingly, the pressure evolution of the shear anisotropy, defined as $A=2(C'-C_{44})/(C'+C_{44})$, is very different for the high-spin and low-spin ferropericlase (see inset of Figure 3): while A increases linearly with pressure in the high-spin phase, it remains almost constant (or slightly decreases) in the low-spin phase. Thus, we suggest that a seismically detectable signature of the spin transition in the lower mantle may be observed in the shear anisotropy. Indeed, since ferropericlase is much weaker than perovskite, it can accommodate most of the strain (31), developing strong texture (32) and possibly controlling the shear anisotropy of the lower mantle. Our measurements indicate a very large shear anisotropy, amounting to approximatively 70% at 70 GPa for ferropericlase with a Fe content x=17 at.%, a value very close to what measured for ferropericlase with x=10 at.% (10, 26), and somewhat larger than that measured for ferropericlase with x=6 at.% (9). Most importantly, this value is at least

50% larger than the shear anisotropy of MgO (26), which is typically used in geodynamical modeling. Such a considerable anisotropy, in conjunction with lattice preferred orientation, strongly argue for ferropericlase as the main phase responsible for the seismic shear anisotropy of the lower mantle.

Finally we point out that the different shear anisotropy behavior of the high-spin and low-spin ferropericlase should be considered together with temperature and chemical variations to interpret local heterogeneities in the lower mantle reported by seismic tomography.

Figures

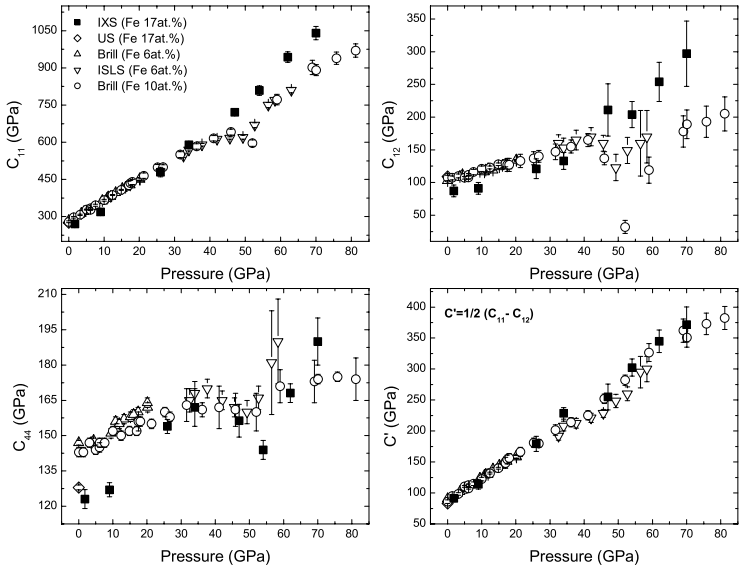

Figure 1: Pressure evolution of the single-crystal elastic moduli of $(Mg_{1-x},Fe_x)O$-ferropericlase. Solid squares: IXS data for x=0.17; open diamonds: ambient pressure ultrasonic determinations for x=0.17 (27); triangles: Brillouin measurements for x=0.6 (25); upsidedown triangles: ISLS results for x=0.6 (9); open circles: Brillouin measurements for x=0.10 (10).

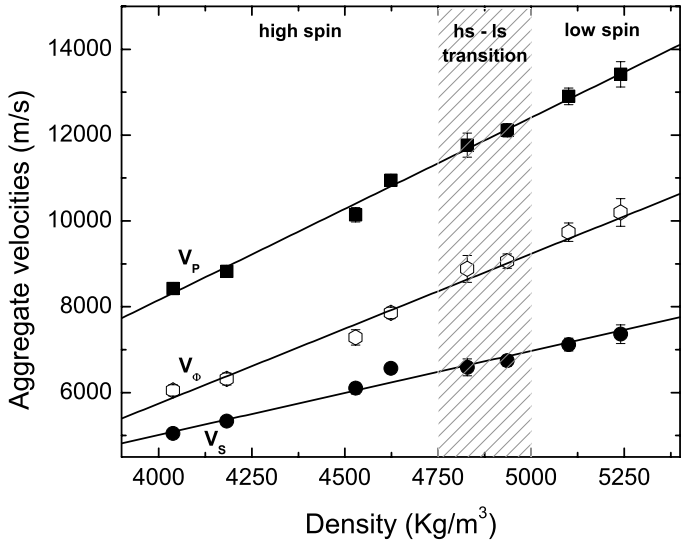

Figure2: Density evolution of the aggregate sound velocities. Solid squares: compressional sound velocity (V_P); solid circles: shear sound velocity (V_S); open hexagons: bulk velocity ($V_\Phi=\sqrt{K/\rho}$). The lines are linear fit to the experimental data. The density range corresponding to the spin transition zone is shaded in gray.

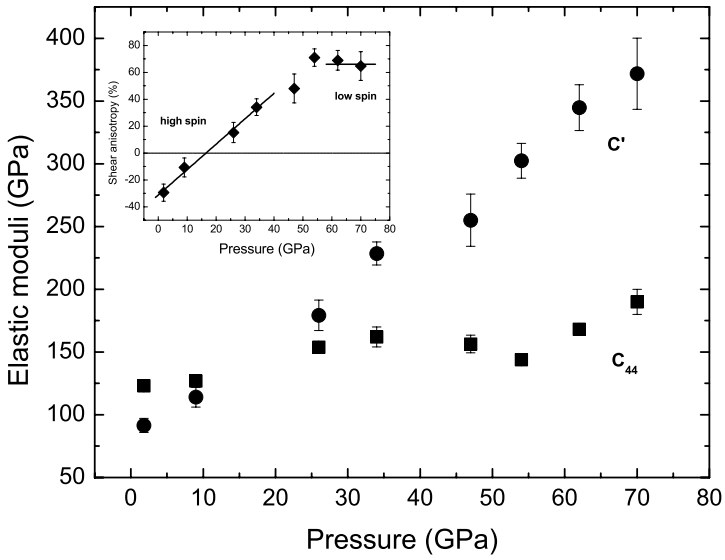

Figure 3: Comparison of the pressure evolution of C_{44} (squares) and C' (circles), corresponding to the two different polarization of the shear mode in the diagonal plane of a cubic lattice. Inset: shear anisotropy as a function of pressure. The lines are guides for the eye.

References

1. J.-P. Poirier, *Introduction to the Physics of the Earth's Interior* (Cambridge University Press, Cambridge, 2000).

2. J. Badro *et al.*, *Science* **300**, 789 (2003).

3. J. Badro *et al.*, *Science* **305**, 383 (2004).

4. J.F. Lin *et al.*, *Nature* **436**, 377 (2005).

5. J.F. Lin *et al.*, *Geophys. Res. Lett.* **33**, L22304 (2006); correction *Geophys. Res. Lett.* **34**, L09301 (2007).

6. S. Speziale *et al.*, *J. Geophys. Res.* **112**, B10212 (2007).

7. K. Catalli *et al.*, *Earth Planet. Sci. Lett.* **289**, 68 (2010).

8. Y. Fei *et al.*, *Geophys. Res. Lett.* **34**, L17307 (2007).

9. J.C. Crowhurst, J.M. Brown, A.F. Goncharov, S.D. Jacobsen, *Science* **319**, 451 (2008).

10. H. Marquardt, S. Speziale, H.J. Reichmann, D.J. Frost, F.R. Schilling, *Earth Planet. Sci. Lett.* **287**, 349 (2009).

11. R.M. Wentzcovitch, *et al.*, *Proc. Natl. Acad. Sci. U.S.A.* **106**, 8447 (2009).

12. J.F. Lin *et al.*, *Science* **317**, 1740 (2007).

13. G. Masters (2008), Eos Trans. AGU, 89(53), Fall Meet. Suppl., Abstract MR23A-04.

14. G. Fiquet, J. Badro, F. Guypt, H. Requardt, M. Krisch, *Science* **291**,468 (2001).

15. D. Antonangeli *et* al., *Earth Planet. Sci. Lett.* **225**, 243 (2004).

16. D. Antonangeli *et* al., *Phys. Rev. B* **72**, 134303 (2005).

17. J. Badro *et al.*, *Earth Planet. Sci. Lett.* **254**, 233 (2007).

18. D. Antonangeli *et al.*, *Earth Planet. Sci. Lett*. **205**, 292 (2010).

19. D. Antonangeli *et al.*, *Phys. Rev. Lett.* **93**, 215505 (2004).

20. D.L. Farber *et al.*, *Phys. Rev. Lett.* **96**, 115502 (2006).

21. D. Antonangeli, M. Krisch, D.L. Farber, D.G. Ruddle, G. Fiquet, *Phys. Rev. Lett.* **100**, 085501 (2008).

22. Materials and methods are available on Science online.

23. J.C. Crowhurst *et al*., *Appl. Phys. Lett.* **89**, 111920 (2006).

24. D.L. Farber, D. Antonangeli, C.M. Aracne, J. Benterou, *High Press. Res.* **26**, 1 (2006).

25. J.M. Jackson *et al.*, *J. Geophys. Res.* **111**, B09203 (2006).

26. H. Marquardt *et al.*, *Science* **324**, 224 (2009).

27. S.D. Jacobsen *et al.*, *J. Geophys. Res.* **107**, 2307 (2002).

28. A.F. Goncharov, V.V. Struzhkin, S.D. Jacobsen, *Science* **321**, 1205 (2006).

29. F. Decremps, L. Nataf, *Phys. Rev. Lett.* **92**, 157204 (2004).

30. L. Nataf, F. Decremps, M. Gauthier, G. Syfosse, *Ultrasonics* **44**, e555 (2006).

31. K. Madi, S. Forest, P. Cordier, M. Boussuge, *Earth Planet. Sci. Lett.* **237**, 223 (2005).

32. C.E. Tommaseo, J. Devine, S. Merkel, S. Speziale, H.K. Wenk, *Phys. Chem. Minerals* **33**, 84 (2006).

33. We acknowledge F. Occelli for his help with the high-pressure cells set up. We wish to thank G. Le Marchand and P. Munsch for gas loading at IMPMC and P. Bouvier, M. Hanfland and M. Mezouar, for gas loading at ESRF. A.L. Auzende is acknowledged for the electron energy loss measurements. This work was performed under the auspices of the U.S. Department of Energy, Lawrence Livermore National Laboratory under Contract DE-AC52-07NA27344 supported by the Office of Basic Energy Sciences – Geosciences Research Program (fjr).

Supporting online material

Materials and Methods

Figs S1 to S4